STUDIES OF THE VERTICAL STRUCTURE MODEL AND THE MICROWAVE ATTENUATION OF CLOUDS AND PRECIPITATION OVER TROPICAL OCEAN AREA*

Zhang Ling (张 凌),

LAGEO, Institute of Atmospheric Physics, Chinese Academy of Sciences, Beijing 100029

Dou Xiankang (窦贤康)

Dept. of Sciences of Earth and Space, University of Science and Technology of China, Hefei 230026

and *Liu Jinli* (刘锦丽)

LAGEO, Institute of Atmospheric Physics, Chinese Academy of Sciences, Beijing 100029

Received November 15, 1997; revised April 15, 1998

ABSTRACT

Using radiosonde data and other related observations in the TOGA-COARE IOP (from November 1, 1992 to February 28, 1993), the microwave attenuation of non-precipitating clouds is investigated based on microwave radiative transfer model (MRTM) at the specific frequencies of 6.8, 10.65, 13.9, 19.35, 22.235, 37.0, 85.5 and 90.0 GHz. Besides, utilizing the data of the airborne radar and radiometer at 13.8 GHz in the IOP (Intensive Observation Period), vertical structure models for different types of precipitating clouds are obtained, and also the microwave attenuation of precipitating cloud is studied. Some statistical characteristics of 13.8 GHz microwave path integrated attenuation for stratiform and convective precipitating clouds are presented. The results given here are valuable for the spaceborne microwave remote sensing of precipitation, and the cloud and precipitation attenuation corrections in the spaceborne microwave remote sensing of earth surface over tropical ocean area.

Key words: spaceborne remote sensing, microwave remote sensing, microwave attenuation

I. INTRODUCTION

In current days the practice of spaceborne microwave remote sensing of geophysical parameters of earth's surface is confined to the atmosphere of clear weather; one of the obstacles that prevent it from being applied to all-weather situation is the correction problem of microwave attenuation due to cloudy and rainy atmospheres. Since clouds and rain in atmospheres are highly inhomogeneous in spatial and temporal scales, and also their observations are scarce in the globe extent, the attenuation correction of clouds and rain remains in research stage. The work given here is the investigation of atmospheric microwave attenuation from clouds and rain during TOGA-COARE IOP (Intensive

* This work was supported by the National Natural Science Foundation of China under the auspices of Major Project Contract No. 49493404 and Project Contract No. 49485006.

Observation Period) through the use of the data of radiosonde, airborne microwave radar and radiometer, and other relevant observations, and in combination with the calculation of microwave radiative transfer model (MRTM). Our purpose is to provide helpful results for the atmospheric attenuation correction in the spaceborne microwave surface sensing over tropical ocean areas.

The important influences of quantitative global precipitation distribution measurements on the changes of globe climates and environments are increasingly being recognized by scientists. To realize the measurement of precipitation distribution over whole global surface in which the 2/3 of total surface are covered by oceans, we can only rely on spaceborne remote sensing in which the passive microwave sensing is an effective tool to measure precipitation from space. In the spaceborne passive precipitation sensing, the relationship between surface precipitation intensity and microwave radiative brightness temperature is required to be established by means of the computation of MRTM. Because the relationship between precipitation intensity and brightness temperature is very sensitive to the vertical cloud structure which is very complicated (Kummerow et al. 1989), the choice of appropriate cloud models in the spaceborne precipitation inversion is greatly important and very difficult. In order to increase the accuracy of spaceborne precipitation sensing, the forming of vertical precipitating cloud structures which are more close to real clouds must be required. With this purpose, the vertical structure of different types of precipitating clouds is statistically investigated through using the airborne radar and radiometer measurement data during TOGA-COARE and some results are obtained. The results presented here are worthy of the research on the spaceborne passive microwave remote sensing of precipitation distribution over tropical ocean areas.

II. MICROWAVE ATTENUATION FROM CLOUDS

The data we will use to calculate the cloud microwave attenuation include the radiosonde data obtained by the Integrated Sounding System (ISS) of NCAR on a Chinese research vessel "Experiment No. 3" located at 2°15′S, 158°E during TOGA-COARE IOP (from November 1, 1992 to February 28, 1993). There are 4 times of release of sonde balloon at 0500, 1100, 1700 and 2300 UT respectively in each day. The sounding instrument is VAISALA RS80-15N radiosonde made in Finland and has a positioning capability through receiving Omega signal besides the measurement of temperature, humidity and pressure that a conventional radiosonde owns. The sounding system outputs a group of average values of meteorological elements in 10 seconds corresponding to an altitude resolution of approximately 50 m.

Besides the radiosonde data, we also use the macro observation records of type and amount of cloud attained by meteorological observers in the same period as that of the radiosonde data. The cloud type, the cloud base height, the cloud top height are determined according to the above observation records. The mean water content in cloud is chosen for every cloud type from the consideration of the radiosonde data, the micro cloud observation records, and the water content measurements in various types of clouds made by airplanes or on high mountains in China and other countries. Three examples of vertical profiles illustrated in Fig. 1 are used for the water content distributions in clouds. The

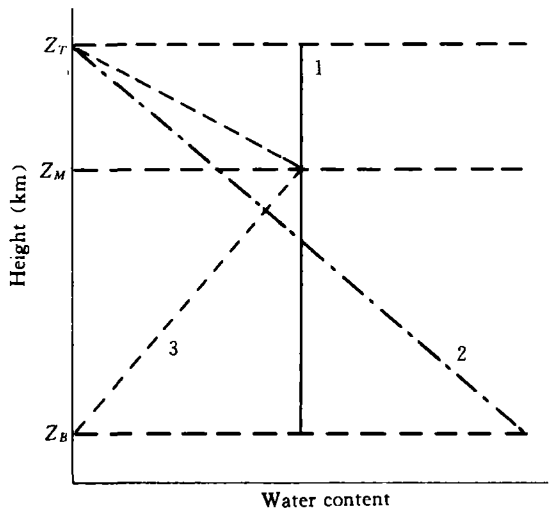

Fig. 1. Three examples of vertical distributions of water content in clouds. Numerals 1, 2 and 3 denote the constant, linear and triangular distributions respectively. There is $Z_M = Z_B + 0.7(Z_T - Z_B)$. Z_T and Z_B are heights of cloud top and bottom, respectively.

Rayleigh scattering model can be employed to calculate the cloud attenuation due to the very small size of cloud droplets in comparison with microwave wavelength.

At first, two sets of cloud samples (low cloud and medium cloud) are obtained from the classification of the whole cloud samples, and then the total path integrated attenuation (PIA, denoted by τ) and the intra-cloud average attenuation coefficient (the total cloud PIA divided by the cloud thickness, which is denoted by α) are calculated for every cloud sample through making use of MRTM, and finally, the statistical parameters of the mean value (represented by E) and the relative RMS deviation (the ratio of the RMS deviation to the mean value, which is represented by σ_R) for the both of τ and α are also calculated for each of the two cloud sample sets. The eight specific frequencies: 6. 8, 10. 65, 13. 9, 19. 35, 22. 235, 37. 0, 85. 5, and 90. 0 GHz, which are commonly employed in spaceborne microwave remote sensing, are selected for the attenuation calculation. Some of our calculation results are recorded in Table 1.

Table 1. The Mean Value E and the Relative RMS Deviation σ_R (%) of the Microwave Cloud Attenuation τ (dB) and the Intra-Cloud Average Attenuation Coefficient α (dB km^{-1}) for Each Set of Cloud Samples. The F and P Mean "Frequency" and "Parameter" Respectively. The Unit of Frequency is GHz.

(a) Low Clouds with a Mean Water Content of 0. 3 g m^{-3}

F	6. 8		10. 65		13. 9		19. 35		22. 235		37. 0		85. 5		90. 0	
P	E	σ_R	E	σ_R	E	σ_R	E	σ_R	E	σ_R	E	σ_R	E	σ_R	E	σ_R
τ	0. 008	42. 4	0. 019	42. 4	0. 033	42. 4	0. 064	42. 4	0. 084	42. 4	0. 227	42. 3	1. 05	41. 6	1. 14	41. 6
α	0. 008	6. 15	0. 019	6. 12	0. 032	6. 10	0. 062	6. 04	0. 082	6. 00	0. 222	5. 71	1. 03	4. 10	1. 12	3. 92

(b) Low Clouds with a Mean Water Content of 0. 2 g m^{-3}

F	6. 8		10. 65		13. 9		19. 35		22. 235		37. 0		85. 5		90. 0	
P	E	σ_R	E	σ_R	E	σ_R	E	σ_R	E	σ_R	E	σ_R	E	σ_R	E	σ_R
τ	0. 005	42. 4	0. 013	42. 4	0. 022	42. 4	0. 042	42. 4	0. 056	42. 4	0. 151	42. 3	0. 698	41. 6	0. 760	41. 6
α	0. 005	6. 15	0. 013	6. 12	0. 022	6. 10	0. 042	6. 04	0. 055	6. 00	0. 148	5. 71	0. 684	4. 10	0. 745	3. 92

(c) Medium Clouds with a Mean Water Content of 0. 1 g m^{-3}

F	6. 8		10. 65		13. 9		19. 35		22. 235		37. 0		85. 5		90. 0	
P	E	σ_R	E	σ_R	E	σ_R	E	σ_R	E	σ_R	E	σ_R	E	σ_R	E	σ_R
τ	0. 008	47. 4	0. 019	47. 4	0. 032	47. 4	0. 061	47. 4	0. 080	47. 4	0. 211	47. 5	0. 829	48. 2	0. 888	48. 3
α	0. 004	12. 1	0. 010	12. 0	0. 017	11. 9	0. 032	11. 6	0. 042	11. 5	0. 109	10. 3	0. 430	4. 72	0. 460	4. 19

(d) Medium Clouds with a Mean Water Content of 0. 05 g m^{-3}

F	6. 8		10. 65		13. 9		19. 35		22. 235		37. 0		85. 5		90. 0	
P	E	σ_R	E	σ_R	E	σ_R	E	σ_R	E	σ_R	E	σ_R	E	σ_R	E	σ_R
τ	0. 004	47. 4	0. 009	47. 4	0. 016	47. 4	0. 031	47. 4	0. 040	47. 4	0. 105	47. 5	0. 415	48. 2	0. 444	48. 3
α	0. 002	12. 1	0. 005	12. 0	0. 008	11. 9	0. 016	11. 6	0. 021	11. 5	0. 055	10. 3	0. 215	4. 72	0. 230	4. 19

It is displayed in Table 1 that the microwave cloud attenuation has the following properties. (1) The mean values of the total cloud attenuation τ and the intra-cloud average attenuation coefficient α are proportional to the mean water content in cloud, and increase with the increasing frequency. (2) In the extent of the chosen frequencies and the chosen mean water contents, the mean value of the total attenuation extends from 0. 005 to 1. 1 dB for low clouds, and from 0. 004 to 0. 9 dB for medium clouds (slightly lower than that of low clouds). (3) In the extent of the chosen frequencies and the chosen mean water contents, the mean value of the intra-cloud average attenuation coefficient extends from 0. 005 to 1. 1 dB km^{-1} for low clouds, and from 0. 002 to 0. 5 dB km^{-1} for medium clouds (higher than low clouds). (4) The relative *RMS* deviation of the total attenuation is 42% for low clouds, and 48% for medium clouds (slightly larger than low clouds). The variation of the total attenuation arises mostly from the scattering of cloud thickness in the cloud sample set. (5) In the extent of the chosen frequencies and the chosen mean water contents, the relative RMS deviation of the intra-cloud average attenuation coefficient extends from 4% to 6% for low clouds, and from 4% to 12% for medium clouds (larger than low clouds). The variation of the intra-cloud average attenuation coefficient arises chiefly from the divergence of cloud height in the cloud sample set.

Moreover, our other calculations manifest that besides relying on the microwave frequency the total microwave cloud attenuation is determined chiefly by the total column cloud water content, but is influenced very little by the vertical distribution of the cloud water content.

III. MICROWAVE ATTENUATION DUE TO PRECIPITATION

The ARMAR radar and radiometer (both use the same frequency; see Durden et al. 1994 for details) of JPL on board NASA DC-8 aircraft, were employed to measure precipitation system over the equatorial Pacific Ocean during TOGA-COARE IOP. The aircraft measurements were made in the period of January and February of 1993 over the area whose latitude and longitude range from 13°S to 1°N and from 153°E to 162°E respectively. An measurement data used for calculating the microwave precipitation attenuation cover a period of around 20 hours corresponding to a travel of about 15000 km and have a amount of around 1 Gbyte data which are saved in about 130 files. Each of the files has about 10 Mbyte data corresponding to a period of 10 minutes. The principal ARMAR characteristics are listed in Table 2. The ARMAR data quality is as follows: (1) the stability of both transmitter and receiver chains is within 0.5 dB; (2) the minimum detectable reflectivity at 10 km range is 10 dBz; (3) the standard deviation of the antenna pointing is approximately 0.5 degrees.

Table 2. Main ARMAR System Parameters

Range resolution (6 dB width)	80 m
Surface horizontal resolution (12 km altitude)	800 m
Swath width	9 km
Frequency (same as TRMM radar)	13.8 GHz
Sampling frequency	10 MHz
ADC resolution	12 bits
Radiometer ΔT per pixel	1 K

The total precipitation attenuation τ can be calculated by means of a surface reference technique (SRT) which is employed in KZS algorithm (Marzoug and Amayenc 1994; Amayenc et al. 1996) to retrieve rain profile from airborne radar measurements. In the SRT the backscattering cross section of surface is assumed to be invariable when precipitation is present and absent, and consequently the difference between the radar measured values of surface cross section with and without precipitation along the radar beam is the total precipitation attenuation. So as to determine the backscattering cross section of ocean surface, the averaging of the radar measured values from ocean surface when there is no precipitation is performed. In order to choose the radar values in no precipitation circumstances, the brightness temperature measured by the radiometer which works simultaneously with the ARMAR radar is selected as a controlling factor, and the condition that the brightness temperature falls into the range from 100 to 145 K is chosen as the criterion condition for no precipitation situation. Our calculations for a number of ARMAR data files indicate that the RMS deviation of backscattering cross section of ocean surface concentrates on the range between 0.3 and 0.7 dB.

The vertical apparent reflectivity cross section from the nadir radar rays and the radiative brightness temperature corresponding to the radar rays are extracted from an ARMAR data file and are plotted in Fig. 2. In Fig. 2a the ordinate is the vertical distance increasing downward, and the two abscissas are the radar ray scan number and the corresponding approximate horizontal distance respectively. In Fig. 2b the ordinate is the brightness temperature, and the abscissa is the scan number. In Fig. 2a it is seen that the contour lines are very dense around 11. 2 km where is the position of ocean surface corresponding to the maximum reflectivity. In Fig. 2a it is also witnessed that there are stratiform precipitation in the area from scan number 50 to 180 where the zero isotherm brightband can be seen at about 5 km height relative to the ocean surface, and convective precipitation in the area from scan number 190 to 250.

According to the precipitation radar echo characteristics (intensity, height, zero

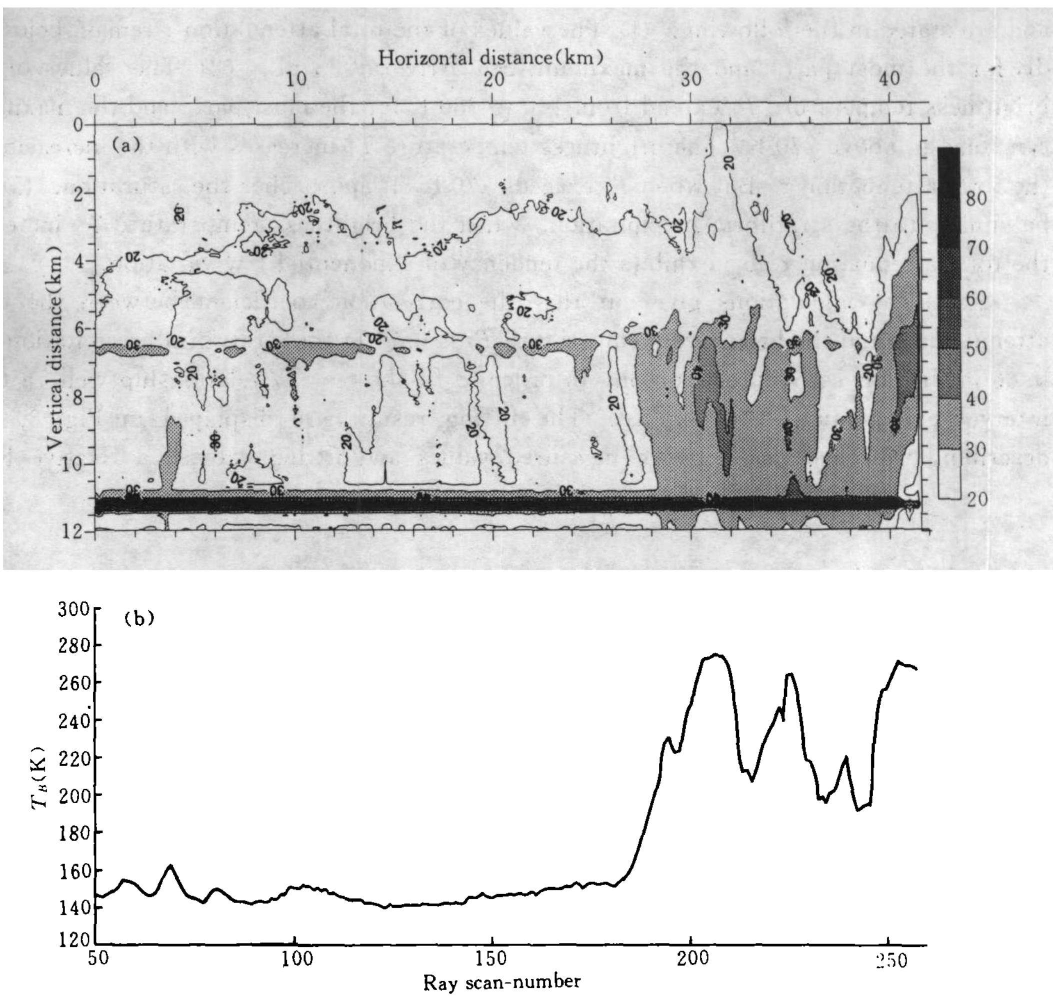

Fig. 2. The graph of the vertical cross section of the ARMAR measured apparent reflectivity and the corresponding brightness temperature distribution along the aircraft track. (a) The apparent reflectivity contour line. The unit of the contour line is dBz. (b) The radiative brightness temperature.

isotherm brightband, scale, etc.), the precipitation is categorized into the two types: stratiform and convective. The attenuation calculations for the stratiform and convective precipitation are separately accomplished. In order to explore the relationship between the total attenuation τ and the brightness temperature T_B, the scatter diagram of τ versus T_B is plotted in Fig. 3.

Some attenuation properties in the stratiform precipitation can be seen in Fig. 3a and are stated in the following. (1) The values of the total attenuation τ lie below 4 dB for the most part, and the maximum can reach 7 dB. (2) The values of the brightness temperature T_B range from 140 to 200 K for the most part, and the maximum can come to 220 K. (3) When the brightness temperature T_B increases the total attenuation τ exhibits a tendency which resembles an exponential law variation.

The attenuation properties in the convective precipitation can also be seen in Fig. 3b and are stated in the following. (1) The values of the total attenuation τ remain below 15 dB for the most part, and the maximum can arrive at 35 dB. (2) The values of the brightness temperature T_B extend from 140 to 260 K for the most part, and the maximum can come to above 270 K. The brightness temperature T_B increases with the increasing of the total attenuation τ. But when T_B exceeds 270 K, it approaches the saturation. (3) To be similar to the stratiform precipitation, when the brightness temperature T_B increases the total attenuation τ also exhibits the tendency of exponential law variation.

Statistical calculations give out that the correlation coefficient between the total attenuation τ and the brightness temperature T_B is 0.71 in the stratiform precipitation and 0.66 in the convective precipitation. In order to fit the $\tau - T_B$ relationship well, a two-interval exponential fit is applied. The fitting results are displayed in Fig. 3. For describing the closeness between measured values and fitting values, a relative RMS

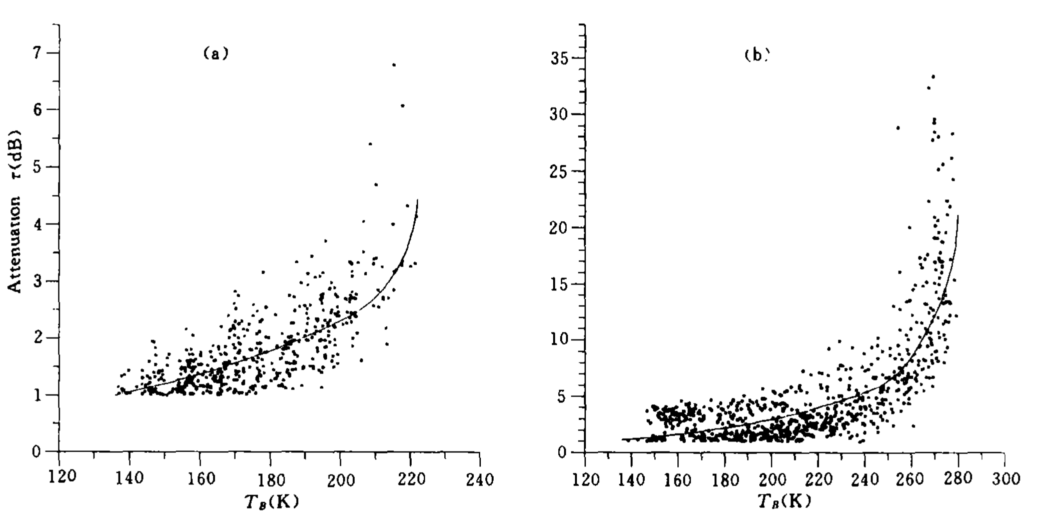

Fig. 3. The scatter plotting of τ versus T_B in the vertical direction and the fitting curve (the solid line) for the $\tau - T_B$ relationship. (a) The stratiform precipitation. There are 501 ray samples. (b) The convective precipitation. There are 775 ray samples.

deviation σ_{RD} between measured values and fitting values of τ is introduced as follows,

$$\sigma_{RD} = 100\left[\frac{1}{N}\sum_{i=1}^{N}\left(\frac{\tau_i - \tau_{Fi}}{\tau_{Fi}}\right)^2\right]^{\frac{1}{2}},$$

where τ_i is the ith measured value of τ, τ_{Fi} is the ith fitting value of τ, N is the number of τ values. The relative RMS deviation σ_{RD} is calculated to be equal to 25% in the stratiform precipitation and 59% in the convective precipitation. The larger deviation σ_{RD} and worse correlation in the convective precipitation than those in the stratiform precipitation indicate that the precipitating cloud structure is more complicated in the convective type than in the stratiform type.

The $\tau - T_B$ relationship obtained here shows that the total microwave precipitation attenuation might be estimated by means of the brightness temperature measurement from spaceborne microwave radiometer.

IV. VERTICAL STRUCTURES OF PRECIPITATING CLOUDS

The same airborne radar and radiometer data as described in Section III are employed to derive vertical structures of precipitating clouds. Several inversion algorithms of single-frequency airborne radar data have been put forward and tested in numerical simulations and radar data inversions (Marzoug and Amayenc 1994; Amayenc et al. 1996). One of these algorithms is the KZS algorithm which is mostly appropriate for the radar data used here. Since the KZS algorithm introduces a constraint of PIA over the range from surface to radar in the radar data inversion, it has the properties of computation stability, wide effective extent (strong, medium, and week precipitation), being not influenced by the vertical cloud structure between the radar location and the initial computation range, and so on.

In order to induce the vertical profiles of precipitating clouds, we firstly classify precipitating clouds into two types: stratiform and convective, and secondly find the ray scan-numbers corresponding to the stratiform and the convective respectively, and then use the KZS algorithm to obtain vertical rain intensity profiles corresponding to every found ray scan-number. The obtained rain profiles are grouped into 6 sets which correspond to 6 grade intervals of surface rainfall rate respectively: 0—3, 3—6, 6—10, 10—20, 20—40, and greater than 40 mm h^{-1}. Finally, the mean value and the relative deviation are calculated for each of the 6 profile sets.

The mean value and the relative RMS deviation of the vertical rainfall intensity profiles are plotted in Fig. 4. From the average vertical profiles in the stratiform precipitation in Fig. 4a, we can find that in the 3 average profiles the rain intensities are quite uniformly distributed below 4 km, and then have a maximum at approximately 4.5 km which is the location of the zero isotherm brightband, and finally decrease as the height increases. Figure 4b suggests that the average vertical profiles in the convective precipitation have the following properties different from those in the stratiform precipitation: (1) in the average profiles of Nos. 1, 2, and 3, the rain intensity is nearly uniformly distributed below 4 km, which is similar to the situation of the stratiform precipitation, and then has a small maximum, which is smaller than that in the stratiform precipitation, at about 4.5 km which is the location of the zero isotherm brightband, and

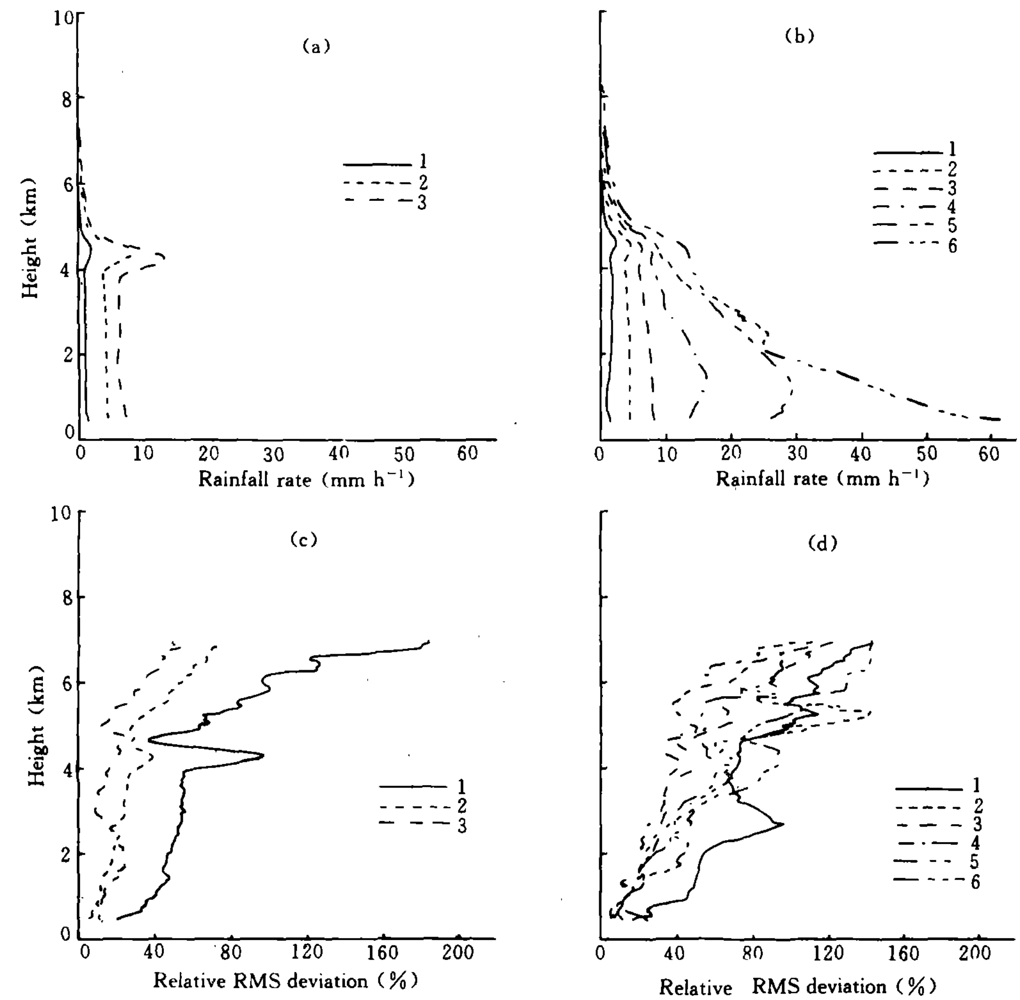

Fig. 4. The vertical profiles of the mean value and the relative RMS deviation of rain intensity. (a) and (c) are for the stratiform precipitation. There are 2301 ray scan-numbers. (b) and (d) the convective precipitation. There are 2099 ray scan-numbers.

at last decreases with height; (2) with the increasing of surface rain intensity in the average profiles of Nos. 4 and 5, a distinct maximum of the rain intensity happens near 1.4 km, whereas the maximum at the zero isotherm brightband begins to disappear; (3) in the average profile of No. 6 the rain intensity has the largest value at sea surface and decreases gradually with the increasing of height. The relative deviation in Figs. 4c and 4d shows that the relative deviation generally increases with the increasing of height and ranges from 10% to 90% below 4 km. Although every rain intensity profile sample varies quite greatly from one to another, the average profile has an evident variation law with the change of the sea surface rain rate.

V. CONCLUSION

The vertical structure and microwave attenuation characteristics of clouds and precipitation over tropical ocean area have been investigated and some lawful results for different types of clouds and precipitation have been presented through the using of radiosonde data, 13.8 GHz airborne radar and radiometer data, and other related meteorological data obtained during the TOGA-COARE IOP. These results will serve as a valuable reference for the algorithm development of the passive spaceborne microwave remote sensing of precipitation and the correction research of the microwave attenuation due to clouds and rain in the spaceborne microwave surface sensing over tropical ocean area.

REFERENCES

Amayenc, P., Diguet, J. P., Marzoug, M. and Tani, T. (1996), A class of single- and dual-frequency algorithms for rain rate profiling from a spaceborne radar, Part II: Tests from airborne radar measurements, *J. Atmos. Oceanic Technol.*, **13**: 142—164.

Durden, S. L., Im, E., Li, F. K., Ricketts, W., Tanner, A. and Wilson, W. (1994), ARMAR: An airborne rain-mapping radar, *J. Atmos. Oceanic Technol.*, **11**: 727—737.

Kummerow, C., Mack, R. A. and Hakkarinen, I. M. (1989), A self-consistency approach to improve microwave rainfall rate estimation from space, *J. Appl. Meteor.*, **28**: 869—884.

Marzoug, M. and Amayenc, P. (1994), A class of single- and dual-frequency algorithms for rain rate profiling from a spaceborne radar, Part I: Principle and tests from numerical simulations, *J. Atmos. Oceanic Technol.*, **11**: 1480—1506.